

Structural characteristics and properties of phase singularities in optical fibers

Dong Sung Lim* and El-Hang Lee

Electronics and telecommunication research institute, Yusung P.O. Box 106, Teajon, KOREA

(Received: July 26, 1997)

The formation of phase singularities in optical fibers is theoretically and experimentally investigated. In particular, their structural characteristics and properties are discussed in relation to guided mode patterns. It is found that except for the fundamental linearly polarized(LP) modes, all the mixed modes displayed phase singularities in the transverse plane. The results in the few mode fiber show that superposition of the LP even and odd modes produces isolated dark points and phase singularities. Phase singularities are found to be of the screw type and of first order. The number of phase singularities linearly increases with the number of guided modes.

I. INTRODUCTION

An important element in pattern formation phenomena is the existence of a well-defined local structure or defect. Dislocations and grain boundaries in connective systems and rolls and spiral patterns in chemical reactions are typical examples of localized structures[1-4]. In optics it has been recently recognized that dark points in optical fields can embed phase singularities (i.e. dislocations in wavefronts) where the phase of the field changes by a multiple of 2π if one circulates a closed loop around the points. The TEM_{01}^* doughnut mode in lasers, for instance, has been treated as a helicoidal wave with a first-order phase singularity[5,6].

The morphology of optical dislocations was originally analyzed by Nye and Berry, who had predicted the existence of dislocations and later provided foundation for the theoretical study of these objects in various waves[7,8]. The results were later extended to scattered speckle patterns by several authors, who demonstrated that the theoretical predictions conformed to experimental measurements[9-11]. Their experimental results showed that an optical field with complex spatial structure can have on average one screw dislocation per speckle spot, the number of positive and negative dislocations being equal. Recently such dislocations were demonstrated by computer aided holographic techniques[12-13]. In lasers different mode families of Gaussian Laguerre modes or Gaussian doughnut modes that arise from the interaction and competition of a set of transverse cavity modes were found to embed phase singularities with different charges. These

singularities are especially arranged in the form of regular crystal like structures and the equiphase lines of the field exhibit a notable similarity to the field line of the electrostatic field generated by a corresponding set of point charges[5]. Similarly the existence of the phase singularities in optical fibers was discussed in 1990 by Bazhenov et. al.[15] and by the Harrison group[16]. More recently, phase singularities have been studied in nonlinear systems as a route to turbulence in spatially complex optical fields[5,14].

The work presented in this paper examines in detail the fundamental properties and structures of phase singularities present in optical fibers. The formation of phase singularities is theoretically and experimentally investigated in several different optical fibers ranging from single mode fiber, through few mode fibers where the pattern consists of several spots, to large core fiber where the transmitted signal shows complicated speckle patterns containing several hundred irregular spots. In section II, the guided mode theory is used to explain the properties of phase singularities in few mode fibers. In section III, experimental arrangements for observing phase singularities in optical fibers are given. In the following sections, experimental results and concluding remarks are given.

II. THEORY OF PHASE SINGULARITIES IN OPTICAL FIBERS

The time and space variation of the total electric field including the transverse variation, as it travels along the z-direction through a optical fiber, can be written as a linear superposition of guided modes in the form

**e-mail : dslim@utopia.etri.re.kr

$$E(r, \phi, z, t) = \sum_k E_k(r, \phi, z) e^{i(\beta_k z - \omega t)} \quad (1)$$

where r and ϕ respectively denote the radial and angular direction in the cylindrical coordinate system. By writing the fields in this fashion, we separate out the plane wave aspects of the wave propagation as given by the $e^{i(\beta_k z - \omega t)}$ factors, where β_k are the eigen propagation constants with respect to the z -direction, and ω is the angular frequency. It is assumed here that the transverse eigen modes of the optical fiber form a complete set. The completeness property means that any arbitrary field pattern inside the fiber can always be expanded using a set of the eigen modes as the basis set. Therefore, the guided modes are essentially plane waves, multiplied by the transverse amplitude profiles given by transverse eigen mode functions $F_k(r, \phi)$;

$$E_k(r, \phi, z) = \frac{1}{2} f_k(z) F_k(r, \phi) + c.c \quad (2)$$

where f_k are the modal amplitudes that are related to the power given to the modes. Although the exact expression of the associated optical beams must necessarily have some small axial E and H field components, the primary field components in those beams are polarized transverse to the direction of propagation in the weakly guiding fibers[17,18]. These waves are referred to as the linearly polarized(LP) modes. For circular core fibers, the angular dependence in the transverse amplitude profiles is through trigonometric functions of either $\cos(l\phi)$ or $\sin(l\phi)$, which are denoted as the LP even or odd modes respectively. The radial component is described by the Bessel functions (J_l) for the core region

$$F_{lmj}(r, \phi) = J_l\left(\frac{ur}{a}\right) \times \begin{cases} \cos(l\phi) & j = 1 \\ \sin(l\phi) & j = 2 \end{cases} \quad (3)$$

and by modified Bessel functions (K_l) for the cladding region

$$F_{lmj}(r, \phi) = \frac{J_l(u)}{K_l(iw)} K_{l+1}\left(\frac{iwr}{a}\right) \times \begin{cases} \cos(l\phi) & j = 1 \\ \sin(l\phi) & j = 2 \end{cases} \quad (4)$$

where a is radius of the core of the fiber and u and w are the transverse propagation constants. Here the index k is replaced by indices lmj where l is the radial index, m is angular index of the mode and j denotes even ($j = 1$) or odd ($j = 2$) modes.

2.1 Single mode fiber

Single mode fibers support only one transverse mode LP₀₁ that exists at all frequencies. For the LP₀₁ mode, the angular dependence of the field is omitted and $l = 0$, so that the transverse mode distribution is described by only the zero order Bessel function J_0 and is given by

$$F_{010}(r, \phi) = J_0\left(\frac{ur}{a}\right). \quad (5)$$

This solution does not possess any dark points in the field distribution and the phase and amplitude are independent of the angular component ϕ . Therefore, no phase singularities are formed in the pattern transmitted by the fiber.

Before continuing, it is important to consider beam propagation in free space, since the beam emerging from an optical fiber is divergent and the wavefronts of the beam are gradually curved as it propagates in free space. The phase of the beam is then expressed as $\Phi(r, z) = kz - k\frac{r^2}{2R(z)}$ where kz is the phase of a plane wave, and $R(z)$ is the radius of curvature of the beam and is responsible for the wavefront bending[19]. This second term represents the deviation of the phase at off-axis points from that at the axial point in a given transverse plane. The radius of curvature subsequently increases with further increase of z until $R(z) \approx z$ for $z \gg z_R$ where z_R is the Rayleigh length. Under the condition, the beam emerging from the fiber at a given plane $z = z_0$ is given by

$$E(r, \phi, z) = f_{010} J_0\left(\frac{ur}{a}\right) \exp(ikz_0 - ik\frac{r^2}{2R(z_0)}), \quad (6)$$

where $R(z_0)$ is the radius of curvature. Now the intensity distribution of the interference pattern produced by overlapping the reference beam with the diverging beam is obtained by taking the square of the sum of the two beams

$$I(r, \phi, z) = E_0^2 + |f_{010}|^2 J_0^2\left(\frac{ur}{a}\right) + 2E_0 |f_{010}| J_0\left(\frac{ur}{a}\right) \cos(\eta r^2), \quad (7)$$

where a new constant η given by $\eta = k/2R(z_0)$. For simplicity, the reference beam was assumed to be a uniform plane wave $\mathbf{E}(r, \phi, z) = E_0 \exp(ikz)$ where k is the propagation constant in free space. Note that the constant η determines the fringe spacing between the two successive maxima in the interference pattern. Fig. 1 b) shows the interference pattern of the LP₀₁ mode for $\eta = 50$. The interference pattern is the usual circular ring fringe. Therefore one can confirm that no phase singularity exists in the single mode solution.

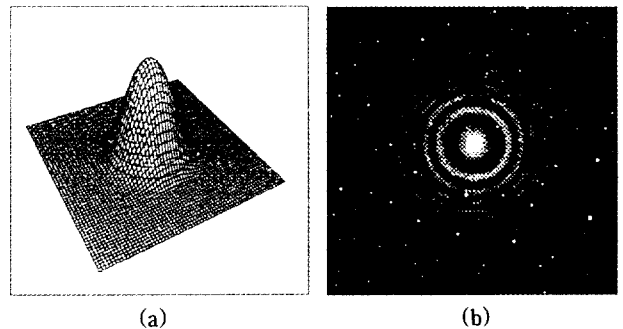


FIG. 1. Calculated intensity mode distribution and circular fringes of a single mode fiber

2.2 Few mode fibers

Two mode fibers can support the next higher order LP modes denoted as even and odd LP₁₁ modes. In this case the solutions for the two modes are described by a first order Bessel function J_1

$$F_{111}(r, \phi) = J_1\left(\frac{u_2 r}{a}\right) \cos \phi, \quad (8)$$

$$F_{112}(r, \phi) = J_1\left(\frac{u_2 r}{a}\right) \sin \phi. \quad (9)$$

In addition, the LP₀₁ mode in the fiber is described by the zero order Bessel function

$$F_{010}(r, \phi) = J_0\left(\frac{u_1 r}{a}\right). \quad (10)$$

The transmitted mode pattern in the fiber is then described by a linear combination of these three modes

$$E(r, \phi) = f_{010}F_{010}(r, \phi) + f_{111}F_{111}(r, \phi) + f_{112}F_{112}(r, \phi). \quad (11)$$

$$E(r, \phi) = J_1\left(\frac{u_2 r}{a}\right) \left[|f_{112}|a \sin \phi + \frac{1}{2}(|f_{111}| + |f_{112}|b)e^{i\phi} + \frac{1}{2}(|f_{111}| - |f_{112}|b)e^{-i\phi} \right]. \quad (12)$$

To understand the formation of the phase singularities one can first consider special cases. When $|f_{111}| = |f_{112}|$, $a = 0$ and $b = +1(-1)$ the patterns have a doughnut intensity distribution with different directions of helical wavefronts given by:

$$E_{110} = |f_{111}|J_1\left(\frac{u_2 r}{a}\right)e^{i\phi}, \quad (13)$$

$$E_{111} = |f_{112}|J_1\left(\frac{u_2 r}{a}\right)e^{-i\phi}. \quad (14)$$

The presence of the factors $e^{\pm i\phi}$ and $J_1(0) = 0$ in the equations confirms the existence of phase singularities at the origin of the patterns, i.e. the phase of the wave changes by 2π with a round trip around the z axis in the x - y plane. These doughnut modes respectively have a positive and negative phase singularity at the center of the patterns. The existence of the phase singularity can be visually confirmed by the interference

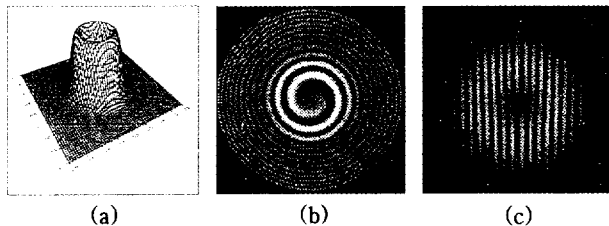


FIG. 2. Phase singularity in two mode fiber; a) intensity distribution of the doughnut mode, b) interference pattern in a circular fringe and c) in a wedge fringe.

Theoretically Eq.(11) implies that one can generate an almost infinite number of possible patterns by varying the complex amplitudes of the three modes.

It is found that the pure LP modes do not produce the phase singularities. The mode distribution of the LP₀₁ mode in the two mode fiber is identical to that of the single mode fiber so that no singularity is formed. Also the LP₁₁ modes cannot embed a phase singularity because the zero intensity region is a line instead of a point. In this case the phase jumps by π on crossing the null line and the wavefronts have the “staggered comb” structure. This structure is a non-localized interference fringe, not a phase singularity. However, we can find the phase singularity in the mixed mode patterns that arise as a result of a linear combination of the LP₁₁ even mode and the LP₁₁ odd mode. To show this, let us consider superposition of the two LP₁₁ modes with the relative phase difference written in a form $e^{i\theta_0} = a + ib$. The field can be written in a form

technique. Consequently, the intensity distribution of the interference patterns is given by

$$I(r, \phi, z) = E_0^2 + |f_{111}|^2 J_1^2\left(\frac{u_2 r}{a}\right) + 2E_0 |f_{111}| J_1\left(\frac{u_2 r}{a}\right) \cos \Phi \quad (15)$$

where $\Phi = \phi - \eta r^2$. The position of the intensity maxima in the interference pattern is now defined by a condition $\cos \Phi = 1$ or $\Phi = 2N\pi$ ($N = 1, 2, 3, \dots$) which describes the spiral structure of the interference patterns (see Fig. 2 b)). The direction of the circulation of the spiral line depends on the sign of charges of the phase singularities. The positive phase singularity shows clockwise rotation of the fringe pattern while the negative phase singularity obtained by performing the following transformation $\phi \rightarrow -\phi$ displays anticlockwise rotation. In addition, when wedge fringes are formed by coinciding the two beams with an angle σ , the cosine term of Eq.(15) for the interference maxima will have a form $\Phi = kx \cos \sigma - \phi$ [13]. Instead of the usual periodic fringes, we observed a grating with dislocation; vanishing of one of the interference fringes takes place at the origin (see Fig. 2 c)).

With an arbitrary phase difference, we can obtain the oval patterns with a single phase singularity formed at the origin of the patterns as shown in Fig. 3. The sign of the phase singularities depend on the phase difference between the two LP₁₁ modes. For $b > 0$ (i.e. $0 < \theta_0 < \pi$) a positive phase singularity is formed and for $b < 0$ (i.e. $\pi < \theta_0 < 2\pi$) a negative phase sin-

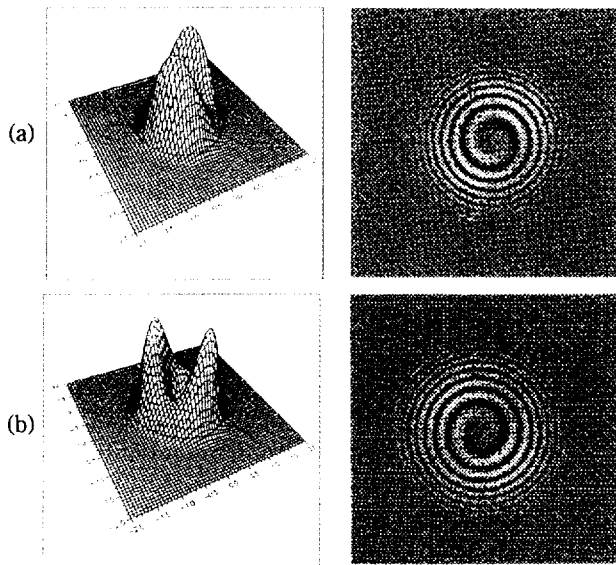


FIG. 3. Intensity distribution of the ovals and their interference patterns in the two mode fiber; a) positive and b) negative charged phase singularity.

gularity is formed. This implies that one can easily transform the sign of a phase singularity by introducing the extra π phase difference between the two LP_{11} modes. Finally, if we consider the patterns resulting from combination of all the three modes, the introduction of the LP_{01} mode results in a displacement of the null point from the center and in turn leads to the relocation of the phase singularity. The location of the phase singularity moves further away from the center as the strength of the LP_{01} mode is increased.

Now we consider the formation of phase singularities in four mode fibers supporting LP_{01} , LP_{11} , LP_{21} and LP_{02} modes. Since the LP_{11} and LP_{21} modes can have even and odd modes the fibers actually support a total of six LP modes. For simplicity only, the three high order LP modes are considered in the following calculation. The LP_{21} even, odd and LP_{02} modes are

$$\tan^{-1} \frac{\text{Im}[E]}{\text{Re}[E]} = \frac{J_2\left(\frac{u_3 r}{a}\right) (|f_{211}| \sin \phi + |f_{212}| (\cos \phi \sin \theta_0 - \sin \phi \sin \theta_0))}{f_{020} J_0\left(\frac{u_4 r}{a}\right) + J_2\left(\frac{u_3 r}{a}\right) (|f_{211}| \cos \phi + |f_{212}| (\cos \phi \cos \theta_0 + \sin \phi \sin \theta_0))}. \quad (21)$$

The cylindrical symmetric patterns ($|f_{020}| \neq 0$ and $|f_{211}| = |f_{212}| = 0$) do not possess any point like phase singularity because the phase does not depend on ϕ . In the case of the doughnut patterns there is one phase singularity located at the center with an associated charge of +2 or -2 depending on whether the fiber supports the E_{211} or E_{212} mode. The equiphase lines of this structure depart radially from the origin and look like the case of the two mode fiber. In this case, if one circulates around the singularity point once, the phase varies by $\pm 4\pi$. On the other hand, the oval patterns, obtained from the superposition of the F_{020} and

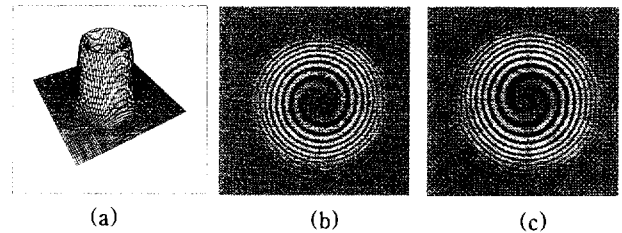


FIG. 4. The doughnut mode with the charge two in four-mode fiber; a) intensity distribution b) positively charged phase singularity c) negatively charged phase singularity.

given by

$$F_{211}(r, \phi) = J_2\left(\frac{u_3 r}{a}\right) \cos(2\phi), \quad (16)$$

$$F_{212}(r, \phi) = J_2\left(\frac{u_3 r}{a}\right) \sin(2\phi), \quad (17)$$

$$F_{020}(r, \phi) = J_0\left(\frac{u_4 r}{a}\right), \quad (18)$$

Again, the combination of LP_{21} even and odd modes with equal amplitudes and a phase difference of $\pi/2$ or $-\pi/2$ between them results in doughnut modes given by

$$E_{211}(r, \phi) = |f_{211}| J_2\left(\frac{u_3 r}{a}\right) e^{2i\phi}, \quad (19)$$

$$E_{212}(r, \phi) = |f_{212}| J_2\left(\frac{u_3 r}{a}\right) e^{-2i\phi}. \quad (20)$$

Fig. 4. shows the intensity mode distribution, and interference patterns of the doughnut modes obtained by overlap of the plane wave. The interference patterns are double helix; two maxima lines spiral out from the origin. If we consider the linear combination of the three modes the intensity mode distributions can be categorically summarized by four distinctive patterns; cylindrical symmetric, doughnut, oval (i.e. the pattern has an elliptical shape with two holes) and four-spotted patterns. To observe the detailed structure of the phase singularities in these patterns the phase map is obtained by calculating a equation given by

E_{211} (or E_{212}) modes with the arbitrary phase difference, possess two separated phase singularities located at the y -axis. The charges of the phase singularities are equal in sign, each amounting to +1 or -1 depending on the doughnut contribution which is dominant in the pattern. When $|f_{020}| < |f_{211}| \approx |f_{212}|$, the patterns are four isolated spots and possess four singularities whose positions are regularly structured. They are placed on the vertices of a square (see Fig. 5 d)) and each of them has a charge equal to either +1 or -1. They are regularly structured in the form of regular geometric arrays. These regularly structured array of

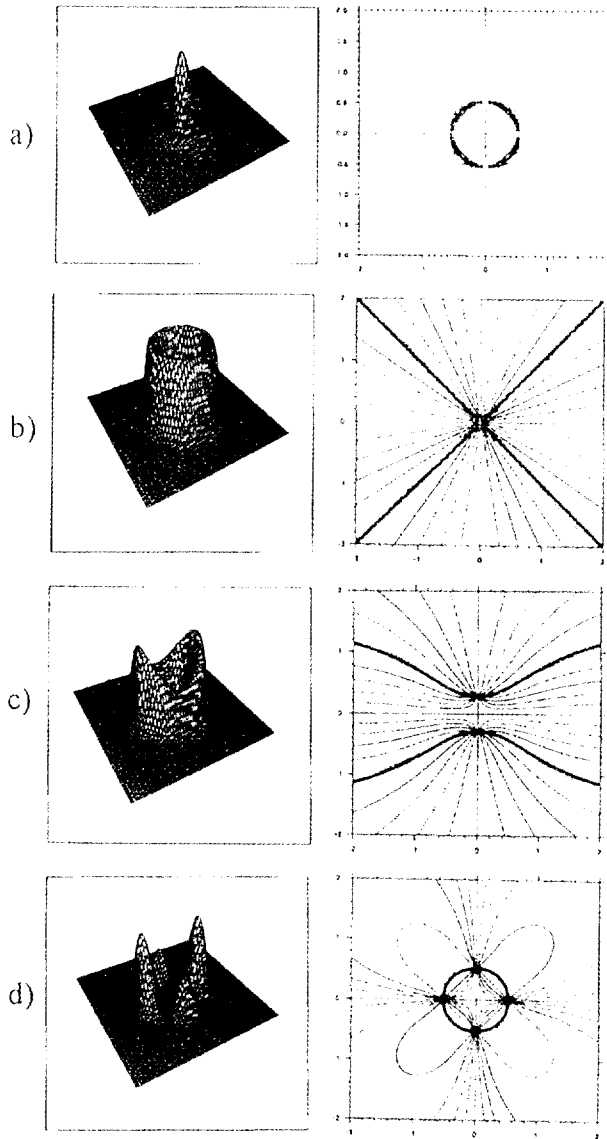


FIG. 5. Calculated intensity mode distribution and phase maps of mode patterns in the four mode fiber. a) cylindrical symmetric, $|f_{020}| = 1.0$ and $|f_{210}| = |f_{211}| = 0$, b) doughnut, $|f_{020}| = |f_{211}| = 0$ and $|f_{210}| = 1.0$ c) oval, $|f_{020}| = 0.5$, $|f_{210}| = 0.5$ and $|f_{211}| = 0$ d) four spotted pattern, $|f_{020}| < |f_{210}| < |f_{211}|$.

phase singularities can be recognized as the lattice of a phase singularity crystal similar to that of laser mode patterns[5].

TABLE 1. Specifications of optical fiber used in the experiments. Numerical aperture(NA), V-parameter and number of LP modes were calculated for 514nm. The length of the fibers was ~ 2 m.

Type of fiber	Core diameter	NA	V- Parameter	Number of LP modes
SM450	$3.1\mu\text{m}$	0.12	2.27	1
SM600	$4.8\mu\text{m}$	0.11	3.23	2
SM1000	$5.5\mu\text{m}$	0.12	4.03	4
SM1300	$9.0\mu\text{m}$	0.11	6.05	6
MMSU	$8.2\mu\text{m}$	0.28	14.03	28
MM	$100\mu\text{m}$	0.12	73	~ 2690

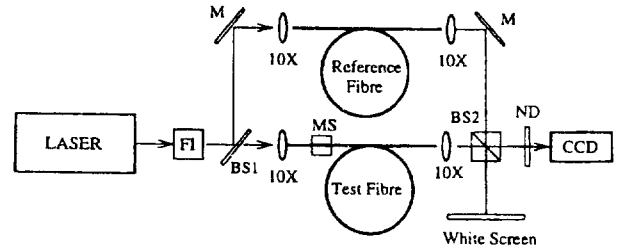


FIG. 6. Experimental set-up for observing phase singularities in optical fibers. FI: Faraday isolator, M: mirrors, BS: beamsplitter, 10times: microscope objective, CCD: CCD camera, MS: mode scrambler.

III. EXPERIMENTAL SET-UP

Fig. 6 shows a schematic diagram of experimental set-up. To visualize the phase singularities hidden in the transverse mode patterns a phase sensitive technique must be used. In these experiments a Mach-Zehnder (MZ) interferometer was employed to monitor phase information of the optical fields. The interferometer was a two-beam amplitude division interferometer constructed by two beamsplitters to divide and recombine the reference and test beams. The light source was an Argon ion laser (Coherent, INOVA 100) operated at a wavelength of 514.5nm, and had a uniform Gaussian transverse mode of TEM_{00} . The linearly polarized laser beam was divided by a beamsplitter(BS1). The transmitted laser beam was then launched into the test optical fiber and the reflected beam was coupled into a short piece of an appropriate single mode fiber (SM450), giving a reference arm of the interferometer. The fiber length used was 1m and typical coupling efficiency into the fiber was found to be 40%. This length was long enough to remove cladding modes (mode patterns of the cladding are similar to those of multimode optical fibers), and thus there was only the guided LP_{01} mode. Details of the optical fibers used in the experiments are shown in Table 1.

IV. EXPERIMENTAL RESULTS

4.1 Single mode fiber

When the V-parameter is smaller than the value 2.405, the fiber only supports a fundamental LP_{01}

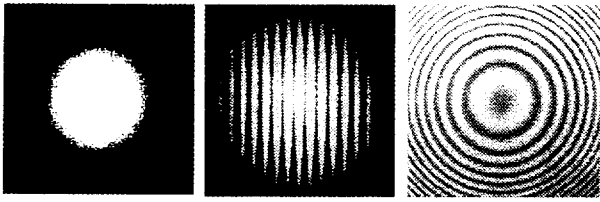


FIG. 7. Intensity distribution and interference patterns in a single mode fibre.

mode. In the experiment, the SM450 fiber matches this condition. The transmitted patterns in the fiber display the LP_{01} mode irrespective of the launching condition. The single mode does not possess any dark points or discontinuities in the intensity mode distribution and no phase singularity was found in the fiber. To confirm the existence of phase singularities, the usual interference techniques were employed. Fig. 7 shows the intensity mode distribution and its corresponding interference pattern in the fiber. As theory predicted, straight interference lines were observed for the wedge fringes and ordinary ring interference patterns for circular fringes.

4.2 Few mode fibers

We begin with a two-mode fiber (SM600) since, as will be shown later, the experimental analysis in the fiber provides a test-bed to confirm the theoretical findings. When LP_{01} mode is dominantly excited in the fiber, no singularity was observed in the transmitted pattern. Furthermore no singularity was found in the pure LP_{11} even and odd modes shown in Fig. 8 a) and b). For the LP_{11} odd mode the localized interference fringe was observed along the null intensity line. Also, the patterns consisting of the two LP_{11} modes with relative phase difference π between two LP_{11} modes did not embed a phase singularity. On the other hand, the doughnut mode, oval or asymmetric two-lobe pattern possess a single phase singularity of charge one. The mixed patterns arising as a result of superposition of the LP_{01} and the two LP_{11} modes displayed asymmetric intensity distribution and the position of phase singularity was located away from the center as shown in Fig. 8 e).

From the theoretical works, we could select either a positive or negative phase singularity by applying a proper phase difference between the LP_{11} even and odd modes. When the light is excited in the LP_{11} even and odd mode with approximately equal amplitude and with the phase difference of $\theta_0 + N\pi$ ($N = 0, 1, 2 \dots$), the interference between the two LP_{11} modes will result in a 90° rotation of pattern and alternation of the charge of the phase singularity for even and odd N 's. Fig. 9 shows the positively and negatively charged phase singularities and their corresponding intensity mode distribution obtained by fine tuning of the launching conditions. This result con-

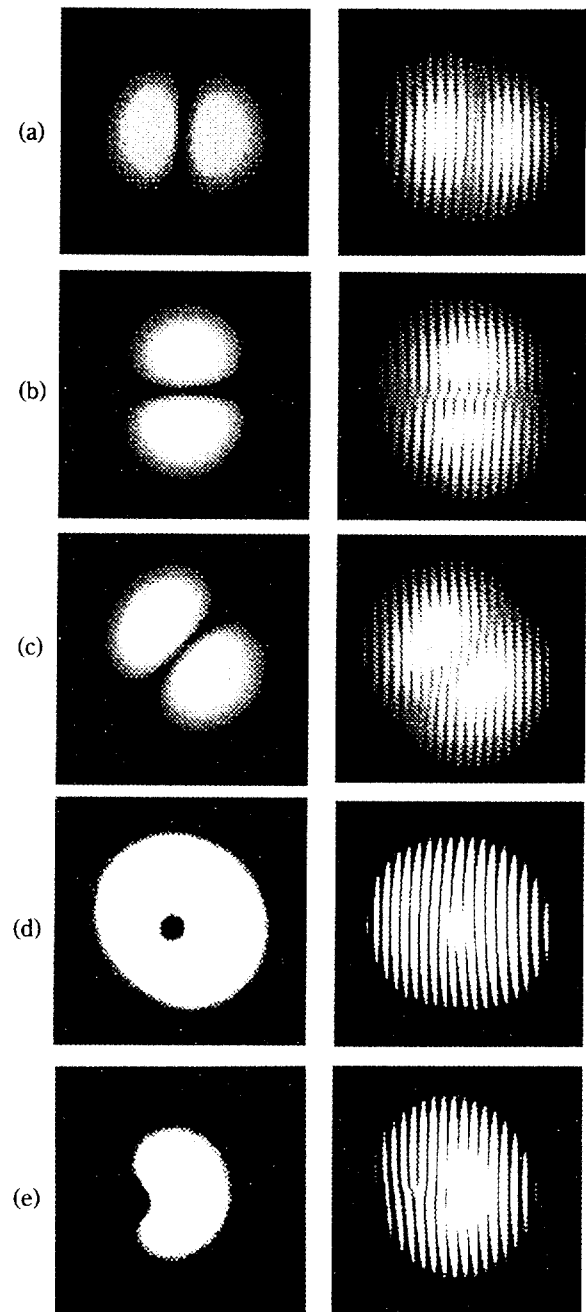


FIG. 8. Phase singularity in two mode fiber a) LP_{11} even mode b) LP_{11} odd mode c) LP_{11} even + odd mode for the initial phase shift $\theta_0 = \pi$ d) doughnut mode e) LP_{01} mode + LP_{11} modes.

firmed the theoretical prediction that the positively charged phase singularity is turned into the negatively charged phase singularity by introducing an extra π phase difference between the two LP_{11} modes (i.e., $(LP_{11} \text{ even}) + (LP_{11} \text{ odd}) \times \exp(\theta_0) \rightarrow (LP_{11} \text{ even}) + (LP_{11} \text{ odd}) \times \exp(\theta_0 + \pi)$).

The maximum number of modes is now increased to four by using a fiber of slightly larger core diameter. A SM100 fiber has V-parameter $V=4.03$ at $\lambda=514\text{nm}$ and

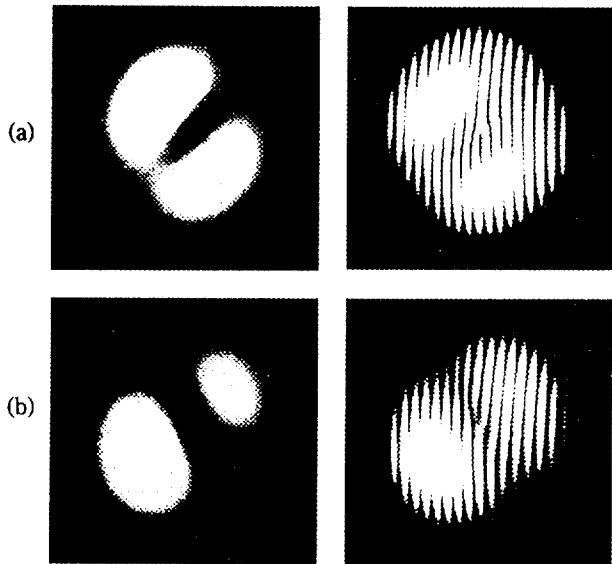


FIG. 9. Positive and negative charged phase singularity and their intensity distribution.

thus supports four LP modes. The maximum number of phase singularity was four although this could be reduced to two or one by varying the launching condition or using a mode scrambler. Fig. 10 shows the phase singularities and their corresponding mode patterns observed in the fiber. For the cylindrical symmetric LP_{02} mode no singularity was observed, but a slight phase distortion appeared at near zero intensity region. A pattern similar to the oval shape displayed two separate positive singularities of charge one. The four-spotted pattern displayed four phase singularities, but their position was not well defined.

The analysis of stability of phase singularities shows that phase singularities with an isolated first order phase singularity are stable with respect to a small perturbation[8]. In the experiment, the formation of the singularities was invariant and stable in the presence of a small perturbation. Furthermore they were always present at all powers investigated, between $\sim 3W$ and $\sim 2mW$ and in fiber lengths ranging from 2.1km to a few centimeters. The singularities were static for fixed launching conditions although the fringes slowly drifted due to environmental disturbances. In addition, although the mixed LP_{21} modes are theoretically known to excite ± 2 charged phase singularities, no phase singularities with topological charge greater than 2 have been observed in experiments, providing possible evidence that the high order phase singularities are unstable due to small perturbations from the environment and, consequently get separated into first order phase singularities. This prediction is further confirmed that the number of phase singularities increased with the complexity of the patterns and thus the number of the guided modes. Fig. 11 plots the total number of phase singularities observed in the various fibers as function of the V - parameter. The total number shows a nearly linear relationship with the number of the LP modes.

The dark region in the intensity distribution can be regarded as an infinite reservoir of phase singularities in which the natural boundaries of the optical beam allow the import and export of phase singularities, thereby limiting the effectiveness of the pairwise creation/annihilation requirement in the few mode fibers. It is in fact true that the total charge ($m_+ + m_-$) of the phase singularities was not preserved in the few

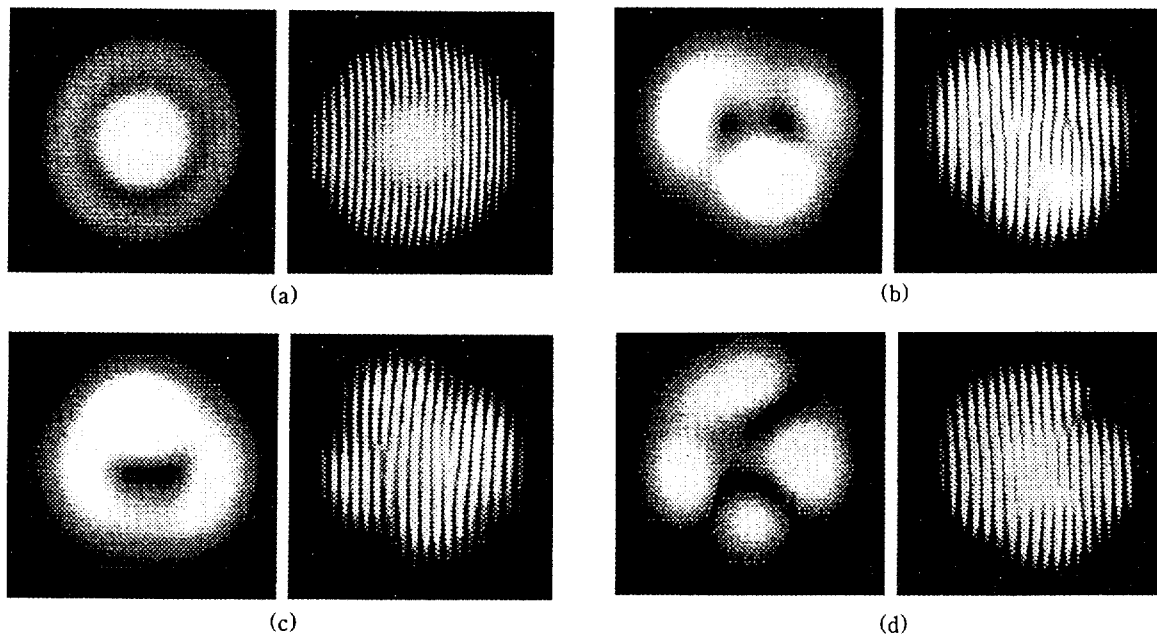


FIG. 10. Phase singularities and their corresponding intensity distribution in a four mode fiber. a) LP_{02} mode b) two opposite charged dislocation c) oval type patterns with two same charged dislocation d) four spotted pattern.

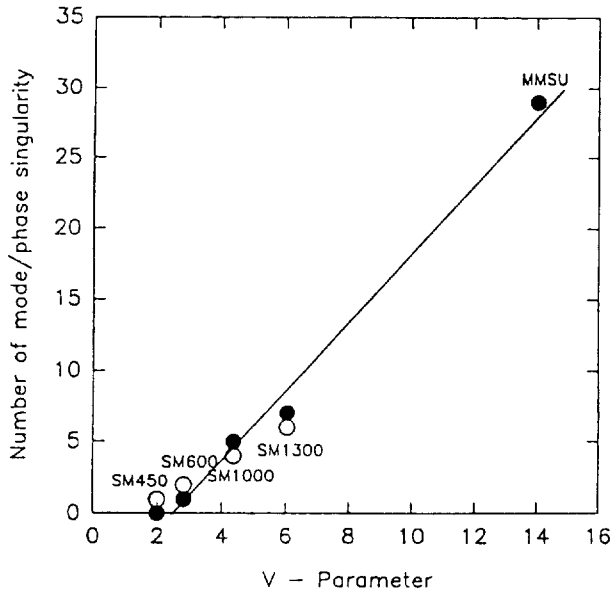


FIG. 11. The maximum number of phase singularities is plotted as function of V-parameter. open circle: number of LP modes and closed circle: number of phase singularities.

mode fibers. This result is consistent with the low Fresnel cavity system studied by Arrechi who proved that the imbalance of total charge normally occurs when the system is strongly dependent on the boundary[20]. In his experiment, it was demonstrated that increasing the size of the aperture inside the cavity, i.e., relaxing the boundary effects, leads to conservation of the total charge. Similarly an increase of core diameter in optical fibers should eventually yield the restriction of boundary effects, so that the paired charges may be conserved. This was indeed the case, as seen in the next section, for very large core fibers, the charge unbalance index $U = |m_+ - m_-|$ becomes very small compared to the total number N of phase singularities.

4.3 Large core fiber

For very large core fibers it is almost impossible to identify the patterns in terms of the waveguide modes. The modes exist in the larger core fibers, but the distinctive features of a single mode are obscured by the large number of modes that become excited under most conditions of illumination. It is therefore easier to analyze such structures as speckle patterns describing a spatially inhomogeneous coherent light field. Practically, the speckle fields are easily generated by interference of a large number of spatially distributed field components reflected from a rough surface[9-10]. In the speckle patterns, the phase and amplitude are both approximately constant within a speckle spot, and different speckle spots are statistically independent. According to Ref[9,10], an optical field with the complex speckle structure can have on average of one phase singularity per speckle spot and the number of positively

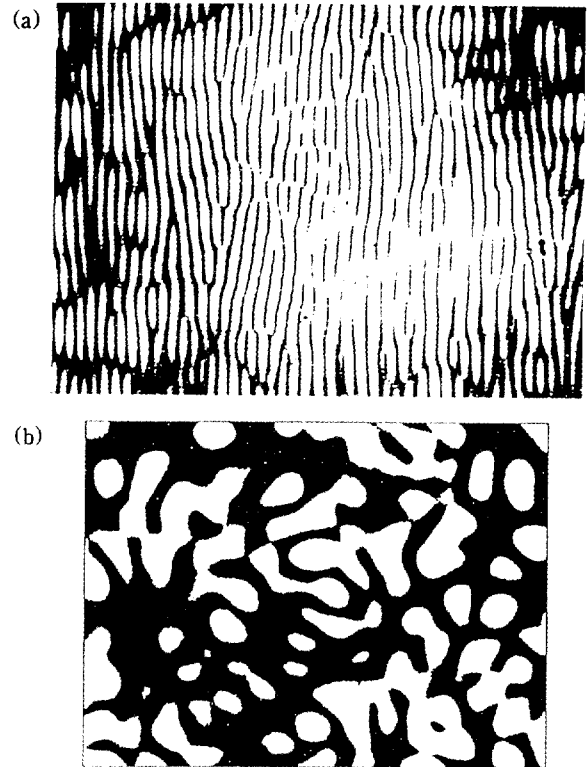


FIG. 12. Intensity distribution and wedge fringes of phase singularities in a MM fiber.

and negatively charged phase singularities is equal.

Fig. 12 shows the center part of a typical mode pattern of the MM fiber and its corresponding phase information. Irrespective of the launching conditions, the transmitted signal through large core (MM, core diameter of $100\mu\text{m}$) fiber displayed very complicated patterns which were characterized by a large number of isolated spots. By carefully comparing these figures one can see that there are usually phase singularities in the dark region. For the case of the long dark strip two oppositely charged phase singularities coexist. However, there were also the dark regions that just create phase distortion of the interference fringes. The total number of phase singularities was found to be comparable to the number of bright spots. In Fig. 12 the total number of the spots was 77 while the total number of phase singularities was 78. In addition, the total number of the two opposite charges was nearly equal, i.e. the unbalance index was much smaller than the total number of phase singularities, i.e., $U=2$ in Fig. 12. We measured the total number of phase singularities (N) on varying the size of a square aperture as shown in Fig. 13. The figure displays the dependence of $N^{1/2}$ on the length of the square aperture (d) i.e. $N^{1/2} \propto d$. This result was consistent with those of the speckle patterns discussed in Ref[9]. We, therefore, conclude that the patterns observed in the large core fiber are within the category of speckle patterns.

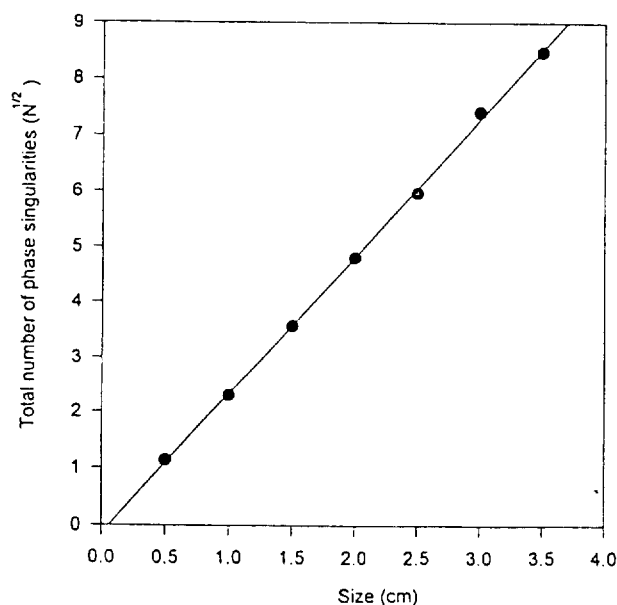


FIG. 13. Number of dislocations(\sqrt{N}) is plotted as function of the length of a square aperture in MM fiber.

V. CONCLUDING REMARKS

In this paper, we have theoretically and experimentally investigated mode patterns and phase singularities in several different optical fibers ranging from single mode fiber to large core fiber. We showed that the phase singularity was a fundamental and essential property of the optical field in multimode optical fibers. Except for the pure LP modes, all the mixed modes displayed phase singularities in the transverse plane. Phase singularities were of the screw type and of first order. The number of phase singularities was found to linearly increase with the number of modes. For analyzing the phase singularities, waveguide mode theory was very useful. A theoretical calculation in the few mode fiber showed that linear superposition of the LP even and odd modes produces isolated dark points and phase singularities in transverse intensity mode distribution (i.e., mixing between the LP even and odd modes was essential). These were found to be in good agreement with experimental results. We also confirmed that excitation for positively and negatively charged phase singularities was critically dependent upon the relative phase difference between the LP₁₁ even and odd modes. For large core fibers, the transmitted signal showed complicated speckle patterns. Their statistics showed that the charge of the phase singularities was nearly conserved and that the total number of phase singularities was comparable to the number of speckles. The total number of phase singularities in the speckle pattern was found to increase linearly with the square of the length of the aperture.

ACKNOWLEDGMENTS

The authors take great pleasure in the acknowledgment of many stimulating discussions with my Prof. R.G. Harrison and Dr. Weiping Lu and Dejin Yu at Heriot-Watt University.

REFERENCES

- [1] "New trends in nonlinear dynamics and pattern forming phenomena: Geometry of nonequilibrium" P. Coulet and P. Huerre, Nato ASI Series B, ed., Physics Vol 237 (Plenum, New York, 1990).
- [2] S.W Morris, E. Bodenscharz, D.S. Cannell and G. Ahlers, Phys. Rev. Lett., **71**, 2026 (1993).
- [3] A.C Newell, Phys. Rev. Lett., **68**, 1864 (1992).
- [4] G.S. Skinner and H.L Swinney, Physica D, **48** 1 (1991).
- [5] M. Brambilla, F. Battipede, L.A. Lugiato, V. Penna, F. Prati, C. Tamm and C.O Wess, Phys. Rev. A **43**, 5090 (1991).
- [6] C.O. Weiss, Phy. Reports, **219**, 311 (1992).
- [7] M.V. Berry, J.F. Nye and F.J. Wright, Phil. Trans. of R. Soc. of London., **291**, 453 (1979).
- [8] M. V. Berry "Singularities in wave and rays" in Physics of defects, ed. by R. Balian ed at. (North Holland publishing company, 1980).
- [9] N. B. Baranova and B. Ya Zel'dovich, Sov. Phys. JETP **53**, 925 (1981).
- [10] N. B. Baranova, B. Ya Zel'dovich, A.V. Mameaev, N.F. Pilipetsky and V.V. Shkunov, Sov. Phys. JETP **56**, 983 (1982).
- [11] B.Ya Zel'dovich, N.F. Pilipetsky V.V. Shkunov, "Principle of phase conjugation" (Springer- Verlag, Berlin, 1985).
- [12] V.Yu. Bazhenov, M.S. Soskin and M. Vasnetsov, J. of Mod. Opt., **39**, 985 (1992).
- [13] I. Basistiy, V. Yu. Bazhenov, M.S. Soskin and M. Vasnetsov, Opt. Comm., **103**, 422 (1993).
- [14] Discussion session after physics report, Phys. Report, **219**, 339 (1992).
- [15] V.Yu. Bazhenov, M.S. Soskin and M.V. Vasnetsov, JEPT Lett. **52**, 429 (1990).
- [16] D.S. Lim, A. Johnstone, Weiping Lu and R.G. Harrison, EQEC 91, Edinburgh, UK (1991).
- [17] D. Gloge, Appl. Opt., **10**, 2252 (1971) .
- [18] D. Marcuse "Theory of dielectric optical waveguides" (Academic press , NY, 1974).
- [19] A. Siegman "Lasers" (University Science Books, Mill Valley, 1986).
- [20] F.T. Arecchi, "Pattern formation and space-time organisation in nonlinear optics" in Nonlinear dynamics and spatial complexity in optical systems, R.G. Harriion and J.S Uppal ed., (Institute of physics publishing, Bristol, 1993) pp. 65-113.